High-order finite element modeling of M1-AWBS nonlocal electron transport

Milan, Vladimir, Philippe, Jean-Luc[a]

[a] *Université de Bordeaux - CNRS - CEA, CELIA, UMR 5107, F-33405 Talence, France*

Abstract

Keywords: Nonlocal transport, Kinetics, MHD, High-order methods, FEM

Contents

1. M1 model

1.1. AWBS Boltzmann transport equation

Simplified Boltzmann transport equation of electrons relying on the use of AWBS collision-thermalization operator [1] reads

$$v\boldsymbol{n}\cdot\nabla f+\frac{q_e}{m_e}\left(\boldsymbol{E}+\frac{v}{c}\boldsymbol{n}\times\boldsymbol{B}\right)\cdot\nabla_{\boldsymbol{v}}f=\nu_e v\frac{\partial}{\partial v}\left(f-f_M\right). \tag{1}$$

1.2. M1-AWBS model

In order to eliminate the dimensions of the transport problem (26) the two moment model referred to as *M1-AWBS* is introduced

$$\begin{aligned}\nu_e v\frac{\partial}{\partial v}\left(f_0-f_M\right) &= v\nabla\cdot\boldsymbol{f}_1+\frac{q_e}{m_e v^2}\boldsymbol{E}\cdot\frac{\partial}{\partial v}\left(v^2\boldsymbol{f}_1\right), &(2)\\ \nu_e v\frac{\partial}{\partial v}\boldsymbol{f}_1-\nu_t\boldsymbol{f}_1 &= v\nabla\cdot\left(\mathbf{A}f_0\right)+\frac{q_e}{m_e v^2}\boldsymbol{E}\cdot\frac{\partial}{\partial v}\left(v^2\mathbf{A}f_0\right)\\ &\quad+\frac{q_e}{m_e v}\boldsymbol{E}\cdot\left(\mathbf{A}-\mathbf{I}\right)f_0+\frac{q_e}{m_e c}\boldsymbol{B}\times\boldsymbol{f}_1, &(3)\end{aligned}$$

where the anisotropy-closure matrix takes the form

$$\mathbf{A}=\frac{1}{3}\mathbf{I}+\frac{|\boldsymbol{f}_1|^2}{2f_0^2}\left(1+\frac{|\boldsymbol{f}_1|^2}{f_0^2}\right)\left(\frac{\boldsymbol{f}_1\otimes\boldsymbol{f}_1^T}{|\boldsymbol{f}_1|^2}-\frac{1}{3}\mathbf{I}\right), \tag{4}$$

which corresponds to the distribution function approximation

$$f=f_0\frac{\left|\boldsymbol{M}_{(\boldsymbol{f}_1/f_0)}\right|}{4\pi\sinh\left(\boldsymbol{M}_{(\boldsymbol{f}_1/f_0)}\right)}\exp\left(\boldsymbol{n}\cdot\boldsymbol{M}_{(\boldsymbol{f}_1/f_0)}\right), \tag{5}$$

where $\boldsymbol{M}_{(\boldsymbol{f}_1/f_0)}\to 0$ when $\boldsymbol{f}_1/f_0\to\mathbf{0}$.

2. High-order finite element scheme

2.1. Variational principle

First, the electro-magnetic scaling

$$\tilde{\boldsymbol{E}}=\frac{q_e}{m_e}\boldsymbol{E},\ \tilde{\boldsymbol{B}}=\frac{q_e}{m_e c}\boldsymbol{B}, \tag{6}$$

is defined in order to make the algebraic operations easier to follow. The general variational formulation of (2) and (3) constructed above the scalar (zero

moment) functional space represented by test functions ϕ and the vector (first moment) functional space represented by test functions $\boldsymbol{w}$ takes the form

$$\int_\Omega \phi \nu_e \frac{\partial f_0}{\partial v} = \int_\Omega \phi \left(\mathbf{I} : \nabla \boldsymbol{f}_1 + \frac{1}{v} \tilde{\boldsymbol{E}} \cdot \frac{\partial \boldsymbol{f}_1}{\partial v} + \frac{2}{v^2} \tilde{\boldsymbol{E}} \cdot \boldsymbol{f}_1 + \nu_e \frac{\partial f_M}{\partial v} \right), \quad (7)$$

$$\int_\Omega \boldsymbol{w} \cdot \nu_e \frac{\partial \boldsymbol{f}_1}{\partial v} = \int_\Omega \boldsymbol{w} \cdot \left(\nabla \cdot (\mathbf{A} f_0) + \frac{1}{v^2} \tilde{\boldsymbol{E}} \cdot (3\mathbf{A} - \mathbf{I}) f_0 + \frac{1}{v} \tilde{\boldsymbol{E}} \cdot \frac{\partial}{\partial v} (\mathbf{A} f_0) + \frac{1}{v} \tilde{\boldsymbol{B}} \times \boldsymbol{f}_1 + \frac{\nu_t}{v} \boldsymbol{f}_1 \right). \quad (8)$$

The corresponding discrete variational principal based on the method of finite elements then reads

$$\int_\Omega \boldsymbol{\phi} \otimes \boldsymbol{\phi}^T \nu_e \, \mathrm{d}\Omega \cdot \frac{\partial \boldsymbol{f}_0}{\partial v} = \int_\Omega \boldsymbol{\phi} \otimes \left(\mathbf{I} : \nabla \mathbf{w}^T + \frac{2}{v^2} \tilde{\boldsymbol{E}}^T \cdot \mathbf{w}^T \right) \mathrm{d}\Omega \cdot \boldsymbol{f}_1 + \int_\Omega \boldsymbol{\phi} \otimes \frac{1}{v} \tilde{\boldsymbol{E}}^T \cdot \mathbf{w}^T \, \mathrm{d}\Omega \cdot \frac{\partial \boldsymbol{f}_1}{\partial v} + \int_\Omega \boldsymbol{\phi} \otimes \boldsymbol{\phi}^T \nu_e \, \mathrm{d}\Omega \cdot \frac{\partial \boldsymbol{f}_M}{\partial v}, \quad (9)$$

$$\int_\Omega \mathbf{w} \cdot \mathbf{w}^T \nu_e \, \mathrm{d}\Omega \cdot \frac{\partial \boldsymbol{f}_1}{\partial v} = - \int_\Omega (\mathbf{A} : \nabla \mathbf{w}) \, \boldsymbol{\phi}^T \, \mathrm{d}\Omega \cdot \boldsymbol{f}_0 + \int_\Omega \mathbf{w} \cdot \frac{1}{v^2} (3\mathbf{A} - \mathbf{I}) \cdot \tilde{\boldsymbol{E}} \, \boldsymbol{\phi}^T \, \mathrm{d}\Omega \cdot \boldsymbol{f}_0 + \int_\Omega \mathbf{w} \cdot \frac{1}{v} \mathbf{A} \cdot \tilde{\boldsymbol{E}} \, \boldsymbol{\phi}^T \, \mathrm{d}\Omega \cdot \frac{\partial \boldsymbol{f}_0}{\partial v} + \int_\Omega \mathbf{w} \cdot \left(\frac{1}{v} \tilde{\boldsymbol{B}} \times \mathbf{w}^T + \frac{\nu_t}{v} \mathbf{w}^T \right) \mathrm{d}\Omega \cdot \boldsymbol{f}_1, \quad (10)$$

where $\boldsymbol{\phi}$ is the finite vector of scalar bases functions, $\mathbf{w}$ is the finite vector of vector bases functions, Ω represents the computational domain, in principle 1D/2D/3D spatial mesh.

2.2. Semi-discrete formulation

In principle, only five following integrators need to be coded to provide a discrete representation (9) and (10), i.e.

$$\boldsymbol{\mathcal{M}}^0_{(g)} = \int_\Omega \boldsymbol{\phi} \otimes \boldsymbol{\phi}^T g \,\mathrm{d}\Omega, \tag{11}$$

$$\boldsymbol{\mathcal{M}}^1_{(g)} = \int_\Omega \mathbf{w} \cdot \mathbf{w}^T g \,\mathrm{d}\Omega, \tag{12}$$

$$\boldsymbol{\mathcal{D}}_{(\mathbf{G})} = \int_\Omega \mathbf{G} : \nabla \mathbf{w} \otimes \boldsymbol{\phi}^T \,\mathrm{d}\Omega, \tag{13}$$

$$\boldsymbol{\mathcal{V}}_{(\boldsymbol{g})} = \int_\Omega \mathbf{w} \cdot \boldsymbol{g} \otimes \boldsymbol{\phi}^T \,\mathrm{d}\Omega, \tag{14}$$

$$\boldsymbol{\mathcal{B}}_{(\boldsymbol{g})} = \int_\Omega \mathbf{w} \cdot \boldsymbol{g} \times \mathbf{w}^T \,\mathrm{d}\Omega. \tag{15}$$

The algebraic representation of the above mathematical objects, which form the basis for numerical discretization, reads

$$\boldsymbol{\phi} = \begin{bmatrix} \phi_1 \\ \vdots \\ \phi_{N_0} \end{bmatrix}, \ \mathbf{w} = \begin{bmatrix} w_{1,1} & \dots & w_{1,d} \\ \vdots & \ddots & \vdots \\ w_{N_1,1} & \dots & w_{N_1,d} \end{bmatrix}, \ \boldsymbol{g} = \begin{bmatrix} g_1 \\ \vdots \\ g_d \end{bmatrix}, \ \mathbf{G} = \begin{bmatrix} G_{1,1} & \dots & G_{1,d} \\ \vdots & \ddots & \vdots \\ G_{d,1} & \dots & G_{d,d} \end{bmatrix}, \tag{16}$$

where d is the number of spatial dimensions, N_0 the number of degrees of freedom of scalar unknown $\boldsymbol{f}_0$, and N_1 is the number of degrees of freedom of vector unknown $\boldsymbol{f}_1$.

Consequently, the discrete analog of M1-AWBS equations (2) and (3) can be written based on (9), (10) as

$$\boldsymbol{\mathcal{M}}^0_{(\nu_e)} \cdot \frac{\partial \boldsymbol{f}_0}{\partial v} - \boldsymbol{\mathcal{M}}^0_{(\nu_e)} \cdot \frac{\partial \boldsymbol{f}_{\boldsymbol{M}}}{\partial v} = \boldsymbol{\mathcal{D}}^T_{(\mathbf{I})} \cdot \boldsymbol{f}_1 + \frac{1}{v} \boldsymbol{\mathcal{V}}^T_{(\tilde{\boldsymbol{E}})} \cdot \frac{\partial \boldsymbol{f}_1}{\partial v} + \frac{2}{v^2} \boldsymbol{\mathcal{V}}^T_{(\tilde{\boldsymbol{E}})} \cdot \boldsymbol{f}_1, \tag{17}$$

$$\begin{aligned} \boldsymbol{\mathcal{M}}^1_{(\nu_e)} \cdot \frac{\partial \boldsymbol{f}_1}{\partial v} - \frac{1}{v} \boldsymbol{\mathcal{M}}^1_{(\nu_t)} \cdot \boldsymbol{f}_1 &= -\boldsymbol{\mathcal{D}}_{(\mathbf{A})} \cdot \boldsymbol{f}_0 \\ &+ \frac{1}{v} \boldsymbol{\mathcal{V}}_{(\mathbf{A} \cdot \tilde{\boldsymbol{E}})} \cdot \frac{\partial \boldsymbol{f}_0}{\partial v} + \frac{1}{v^2} \boldsymbol{\mathcal{V}}_{((3\mathbf{A} - \mathbf{I}) \cdot \tilde{\boldsymbol{E}})} \cdot \boldsymbol{f}_0 + \frac{1}{v} \boldsymbol{\mathcal{B}}_{(\tilde{\boldsymbol{B}})} \cdot \boldsymbol{f}_1, \end{aligned} \tag{18}$$

where the integrators (11), (12), (13), (14), (15) are used acting on appropriate functions ρ, ν_e, ν_t, vectors $\tilde{\boldsymbol{E}}$, $\tilde{\boldsymbol{B}}$, and matrices $\mathbf{A}$ and $\mathbf{I}$.

2.3. Explicit fully-discrete scheme

The easiest way to define a fully discrete scheme is to apply the explicit integration in time, e.g. RK4. Because of the use of different finite element spaces for zero and first moment, and a consequent difficulties of "mass" inversion, a modified two-step explicit scheme is used.

In the first step the time evolution of zero moment quantity $\boldsymbol{f}_0$ is computed as

$$\left(\boldsymbol{\mathcal{M}}^0_{(\nu_e)} - \boldsymbol{\mathcal{M}}^0_{\left(\frac{1}{v\boldsymbol{f}_0^n}\tilde{\boldsymbol{E}}^T\cdot\boldsymbol{f}_1^n\right)}\right)\cdot\frac{\mathrm{d}\boldsymbol{f}_0}{\mathrm{d}v}^* = \boldsymbol{\mathcal{D}}^T_{(\mathbf{I})}\cdot\boldsymbol{f}_1^n + \frac{2}{v^2}\boldsymbol{\mathcal{V}}^T_{(\tilde{\boldsymbol{E}})}\cdot\boldsymbol{f}_1^n + \boldsymbol{\mathcal{M}}^0_{(\nu_e)}\cdot\frac{\partial\boldsymbol{f}_{\boldsymbol{M}}}{\partial v}, \tag{19}$$

where the actual evolution of $\boldsymbol{f}_1$ has been redefined as similar to the time evolution of $\boldsymbol{f}_0$ (compare (19) to (17)). Then, the actual computation of the time evolution of $\boldsymbol{f}_1$ follows

$$\begin{aligned}\boldsymbol{\mathcal{M}}^1_{(\nu_e)}\cdot\frac{\mathrm{d}\boldsymbol{f}_1}{\mathrm{d}v} = &-\boldsymbol{\mathcal{D}}_{(\mathbf{A})}\cdot\boldsymbol{f}_0^n + \frac{1}{v}\boldsymbol{\mathcal{V}}_{(\mathbf{A}\cdot\tilde{\boldsymbol{E}})}\cdot\frac{\mathrm{d}\boldsymbol{f}_0}{\mathrm{d}v}^* \\ &+ \frac{1}{v^2}\boldsymbol{\mathcal{V}}_{((3\mathbf{A}-\mathbf{I})\cdot\tilde{\boldsymbol{E}})}\cdot\boldsymbol{f}_0^n + \frac{1}{v}\boldsymbol{\mathcal{B}}_{(\tilde{\boldsymbol{B}})}\cdot\boldsymbol{f}_1^n + \frac{1}{v}\boldsymbol{\mathcal{M}}^1_{(\nu_t)}\cdot\boldsymbol{f}_1^n.\end{aligned} \tag{20}$$

The superscript n stands for quantities from the previous level of velocity.

As can be seen in FIG. 2.7 we get a heat flux profile corresponding to temperature and density profiles computed by Laghos [2] in 1D and we have also double checked the numerical scheme in 2D and 3D, where apparently the flux profiles exhibit the same physical background. It is important to note, that the current implementation does not include neither electric or magnetic field ($\tilde{\boldsymbol{E}}$, $\tilde{\boldsymbol{B}}$).

It is worth mentioning, that the proposed discrete scheme (19) and (20) naturally obeys the CFL condition with respect to the mesh smallest cell size/mean-stopping-power, and consequently, we needed 8858 energy groups in 1D, 4348 energy groups in 2D, and 10030 energy groups in 3D. This would make the hydro simulation to take more than 1000x longer than classical (SH) hydro.

2.4. Physical analysis of the diffusive asymptotics

The equilibrium (maximized entropy) distribution

$$f_M = \frac{\rho}{v_{th}^3 \left(2\pi\right)^{3/2}} \exp\left(-\frac{v^2}{2v_{th}^2}\right), \tag{21}$$

where $v_{th} = \sqrt{k_B T/m_e}$.

$$\begin{aligned} \frac{\partial f_M}{\partial v} &= -\frac{v}{v_{th}^2} f_M, \\ \frac{\partial f_M}{\partial \rho} &= \frac{1}{\rho} f_M, \\ \frac{\partial f_M}{\partial T} &= \left(\frac{v^2}{2v_{th}^2} - \frac{3}{2}\right) \frac{1}{T} f_M. \end{aligned} \tag{22}$$

The BGK equation, valid for highly isotropic transport, represents the simplest form of the Boltzmann transport equation

$$\boldsymbol{n} \cdot \nabla f + \boldsymbol{n} \cdot \tilde{\boldsymbol{E}} \frac{1}{v} \frac{\partial f}{\partial v} = \frac{(f_M - f)}{\lambda} + \frac{(f_0 - f)}{\tilde{\lambda}}, \tag{23}$$

where $\lambda = \frac{v}{\nu_e} = \frac{v^4}{\sigma\rho}$ is the mean free path expressed as inverse of collisional frequency multiplied by particle velocity, $\tilde{\lambda} = \frac{\lambda}{\alpha}$ is a scattering mean free path expressed as α factor of λ, and f_0 is the isotropic part of the distribution function, thus making the scattering operator being conservative.

The Chapman-Enskog based small parameter (λ) approximation $f \approx f_0 + \lambda f_1 + O(\lambda^2)$ expressed as

$$\boldsymbol{n} \cdot \nabla(f_0 + \lambda f_1) + \boldsymbol{n} \cdot \tilde{\boldsymbol{E}} \frac{1}{v} \frac{\partial f_0 + \lambda f_1}{\partial v} = \frac{(f_M - (f_0 + \lambda f_1))}{\lambda} - \alpha f_1, \tag{24}$$

tells us, that

$$\begin{aligned} f_0 &= f_M, \\ f_1 &= -\boldsymbol{n} \cdot \left(\nabla f_0 + \tilde{\boldsymbol{E}} \frac{1}{v} \frac{\partial f_0}{\partial v}\right) \frac{1}{1+\alpha} = -\boldsymbol{n} \cdot \left(\nabla f_M + \tilde{\boldsymbol{E}} \frac{1}{v} \frac{\partial f_M}{\partial v}\right) \frac{1}{1+\alpha}, \end{aligned}$$

which means, that the localized approximation of the distribution function should behave as

$$\begin{aligned} f \approx f_M - \frac{\lambda}{1+\alpha} \boldsymbol{n} \cdot \left(\nabla f_M + \tilde{\boldsymbol{E}} \frac{1}{v} \frac{\partial f_M}{\partial v}\right) = \\ f_M \left(1 - \frac{\lambda}{1+\alpha} \boldsymbol{n} \cdot \left(\frac{\nabla \rho}{\rho} + \left(\frac{v^2}{2v_{th}^2} - \frac{3}{2}\right) \frac{\nabla T}{T} - \frac{\tilde{\boldsymbol{E}}}{v_{th}^2}\right)\right). \end{aligned} \tag{25}$$

2.5. Physical analysis of the diffusive asymptotics of AWBS

The AWBS equation, valid for fast particle transport, represents one of the simplest forms of the Boltzmann transport equation

$$v\boldsymbol{n}\cdot\nabla f+\boldsymbol{n}\cdot\tilde{\boldsymbol{E}}\frac{\partial f}{\partial v}=v\nu_e\frac{\partial}{\partial v}\left(f-f_M\right)+\nu_t\left(f_0-f\right), \tag{26}$$

where $\nu_e=\frac{\sigma\rho}{v^3}$ is the collisional frequency and $\nu_t=\alpha\nu_e$ is the scattering collisional frequency expressed as α factor of the collisional frequency. We can further proceed by writing the AWBS transport equation in terms of mean free path as

$$\boldsymbol{n}\cdot\nabla f+\boldsymbol{n}\cdot\tilde{\boldsymbol{E}}\frac{1}{v}\frac{\partial f}{\partial v}=\frac{v}{\lambda}\frac{\partial}{\partial v}\left(f-f_M\right)+\frac{\alpha}{\lambda}\left(f_0-f\right), \tag{27}$$

The Chapman-Enskog based small parameter (λ) approximation $f\approx f_0+\lambda f_1+O(\lambda^2)$ expressed as

$$\boldsymbol{n}\cdot\nabla(f_0+\lambda f_1)+\boldsymbol{n}\cdot\tilde{\boldsymbol{E}}\frac{1}{v}\frac{\partial f_0+\lambda f_1}{\partial v}=\frac{v}{\lambda}\frac{\partial}{\partial v}\left(((f_0+\lambda f_1))-f_M\right)-\alpha f_1, \tag{28}$$

tells us, that

$$\begin{aligned}\frac{\partial f_0}{\partial v} &= \frac{\partial f_M}{\partial v}\rightarrow f_0=f_M,\\ f_1 &= -\left(\boldsymbol{n}\cdot\left(\nabla f_0+\tilde{\boldsymbol{E}}\frac{1}{v}\frac{\partial f_0}{\partial v}\right)-v\frac{\partial f_1}{\partial v}\right)\frac{1}{\alpha},\end{aligned}$$

which means, that the localized approximation of the distribution function should behave as

$$\begin{aligned}f\approx f_M-\frac{\lambda}{\alpha}\boldsymbol{n}\cdot\left(\nabla f_M+\tilde{\boldsymbol{E}}\frac{1}{v}\frac{\partial f_M}{\partial v}\right)+\frac{v\lambda}{\alpha}\frac{\partial f_1}{\partial v}=\\ f_M\left(1-\frac{\lambda}{\alpha}\boldsymbol{n}\cdot\left(\frac{\nabla\rho}{\rho}+\left(\frac{v^2}{2v_{th}^2}-\frac{3}{2}\right)\frac{\nabla T}{T}-\frac{\tilde{\boldsymbol{E}}}{v_{th}^2}\right)\right)+\frac{v\lambda}{\alpha}\frac{\partial f_1}{\partial v}.\end{aligned} \tag{29}$$

In order to ensure the plasma to be quasi-neutral, the zero-current condition

$$\boldsymbol{j}=\int_0^\infty\int_{4\pi}q_e v\boldsymbol{n}f\,\mathrm{d}\boldsymbol{n}\;v^2\;\mathrm{d}v=\boldsymbol{0}, \tag{30}$$

can be achieved by providing a consistent electric field in (29), i.e.

$$\tilde{\boldsymbol{E}}=\frac{v_{th}^2\;\int_{4\pi}\boldsymbol{n}\otimes\boldsymbol{n}\cdot\int_0^\infty vf_M\frac{\lambda}{\alpha}\left(\frac{\nabla\rho}{\rho}+\left(\frac{v^2}{2v_{th}^2}-\frac{3}{2}\right)\frac{\nabla T}{T}\right)v^2\,\mathrm{d}v\,\mathrm{d}\boldsymbol{n}}{\int_{4\pi}\boldsymbol{n}\otimes\boldsymbol{n}\cdot\int_0^\infty vf_M\frac{\lambda}{\alpha}v^2\,\mathrm{d}v\,\mathrm{d}\boldsymbol{n}}, \tag{31}$$

which may be further simplified as

$$\tilde{\boldsymbol{E}} = \frac{\int_0^\infty f_M \frac{1}{2}\frac{\nabla T}{T} v^9 \,\mathrm{d}v}{\int_0^\infty f_M v^7 \,\mathrm{d}v} + v_{th}^2 \left(\frac{\nabla \rho}{\rho} - \frac{3}{2}\frac{\nabla T}{T} \right) = v_{th}^2 \left(\frac{\nabla \rho}{\rho} + \frac{5}{2}\frac{\nabla T}{T} \right), \qquad (32)$$

where it is worth mentioning, that the part $f_M + \frac{v\lambda}{\alpha}\frac{\partial f_1}{\partial v}$ of the distribution does not contribute to the current since it is isotropic. One can write the quasi-neutral distribution function explicitly distinguishing between original part (blue color) and E field correction (red color) as

$$f \approx f_M \left(1 - \frac{\lambda}{\alpha} \boldsymbol{n} \cdot \left(\frac{v^2}{2v_{th}^2} - \frac{3}{2} - \frac{5}{2} \right) \frac{\nabla T}{T} \right) + \frac{v\lambda}{\alpha}\frac{\partial f_1}{\partial v}. \qquad (33)$$

which leads to the resulting heat flux

$$\boldsymbol{q}_H = \int_{4\pi}\int_0^\infty \frac{m_e v^2}{2} v \boldsymbol{n} f v^2 \,\mathrm{d}v \,\mathrm{d}\boldsymbol{n} = \frac{4\pi}{3}\frac{m_e}{2}\frac{1}{\alpha\sigma\rho}\int_0^\infty \left(\frac{v^2}{2v_{th}^2} - \frac{3}{2} - \frac{5}{2} \right) v^9 f_M \,\mathrm{d}v \frac{\nabla T}{T}.$$

Based on the Gauss integral formula

$$\int v^{2s+1} \exp\left(-\frac{v^2}{2v_{th}^2} \right) \,\mathrm{d}v = \frac{s!\,(2v_{th}^2)^{s+1}}{2}$$

and Maxwell-Boltzmann distribution (21) the heat flux can be written as

$$\boldsymbol{q}_H = \frac{4\pi}{3}\frac{m_e}{2}\frac{1}{\alpha\sigma\rho}\frac{\rho}{v_{th}^3\,(2\pi)^{3/2}}\frac{4!\;2^4 v_{th}^{10}}{T}\left(5 - \frac{3}{2} - \frac{5}{2} \right)\nabla T = \frac{m_e}{\alpha\sigma}\frac{128}{\sqrt{2\pi}}\left(\frac{k_B}{m_e} \right)^{\frac{3}{2}} T^{\frac{5}{2}} \nabla T. \qquad (34)$$

In conclusion, equation (34) provides nothing else than the well known Lorentz approximation heat flux and its nonlinearity 2.5 in temperature. What is worth mentioning is the effect of E field (quasi-neutrality), which reduces the flux of about 71.4% (also assuming constant density).

2.6. AWBS diffusive asymptotic nonlinearity check

$$\boldsymbol{q}_1 = a_1\, T_1^\alpha\, \nabla T_1, \quad \boldsymbol{q}_0 = a_0\, T_0^\alpha\, \nabla T_0,$$

where we keep $a_1 = a_0 = a$ and $\nabla T_1 = \nabla T_0 = \nabla T$ to be equal in every point of the computational domain. The ration of the fluxes than provides a very important information about flux nonlinearity

$$\frac{\boldsymbol{q}_1}{\boldsymbol{q}_0} = \frac{a\, T_1^\alpha\, \nabla T}{a\, T_0^\alpha\, \nabla T} = \left(\frac{T_1}{T_0} \right)^\alpha,$$

where the nonlinearity is better expressed as

$$\alpha = \frac{\log\left(\frac{\boldsymbol{q}_1}{\boldsymbol{q}_0}\right)}{\log\left(\frac{T_1}{T_0}\right)} \tag{35}$$

Finally, based on the simulation results of two runs corresponding to temperature T_0 with the mean $T = 1000$ executed as

```
mpirun -np 8 nth -p 5 -m data/segment01.mesh -rs 6 -tf 0.0 -ok 4 -ot 3
                                  -vis -fa -print -Tmax 1050 -Tmin 950 -a0 1e12,
```

and to temperature T_1 with the mean $T = 1100$ executed as

```
mpirun -np 8 nth -p 5 -m data/segment01.mesh -rs 6 -tf 0.0 -ok 4 -ot 3
                                  -vis -fa -print -Tmax 1150 -Tmin 1050 -a0 1e12,
```

we got the following numbers

$$\boldsymbol{q}_1 = 0.0891,\ \boldsymbol{q}_0 = 0.0703,\ T_1 = 1100,\ T_0 = 1000,$$

which provide the corresponding nonlinearity

$$\alpha = 2.486487132294661. \tag{36}$$

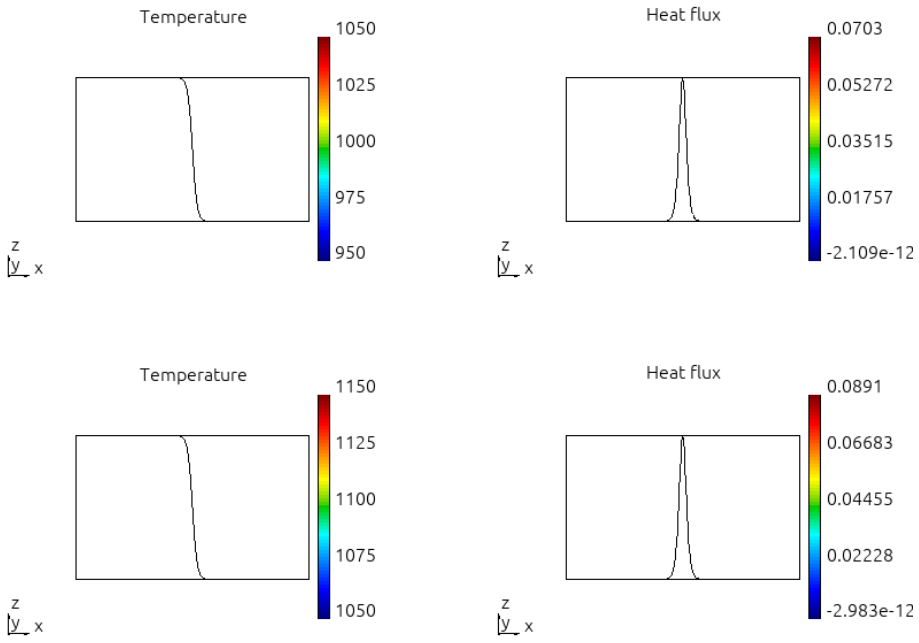

Figure 1: Problem 5 - AWBS nonlinearity check.

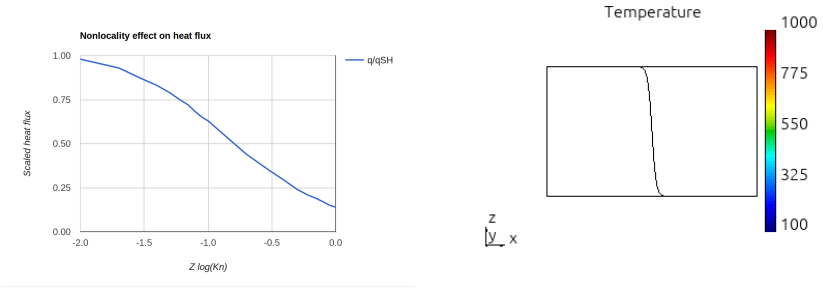

Figure 2: M1-AWBS model. Left: The maximum of computed flux normalized with respect to the value of SH flux. E field effect is not included. Right: Corresponding temperature profile. Density and ionization (scattering on Z = 100 included) have been kept constant.

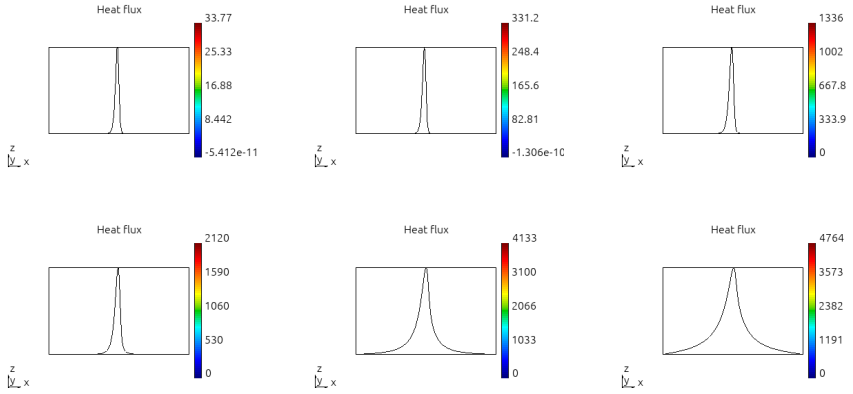

Figure 3: Heat flux calculated by M1-AWBS model. Figures in left-right top-bottom order correspond to Kn = 0.001, 0.01, 0.05, 0.1, 0.5, 1.0. E field effect is not included. Density and ionization (Z = 100) have been kept constant.

Some observations:

- Our calculated distribution function is thermalized, i.e. $f_0 = f_M$.
- With added scattering we also obtain the correct value of calculated heat flux, i.e. $q = q_{SH}$, nevertheless, this works with no E field.

- The E field effect is implemented. When tested with the analytic formula $E_{SH} = v_{th}^2(\nabla ne/ne + 5/2 nabla T/T)$ (we consider Z=100), the corresponding flux reduction due to E field is also correct (flux is reduced to 30% of its E=0 value).

- However, the E_{SH} does not work under any condition, i.e. it exhibits some extra dependence on temperature.

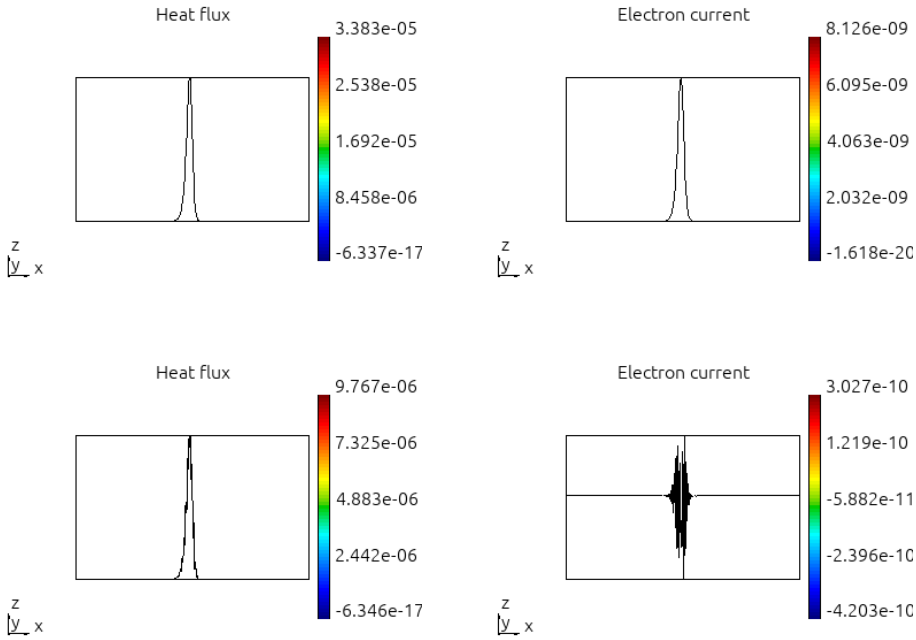

Figure 4: Preliminary results with respect to the E field effect. The SH analytic formula for E field leads to the corresponding current reduction ($j \approx 0$). The corresponding heat flux is reduced $\approx$ by 70 %, exactly as predicted. Nevertheless, the formula exhibits some dependence on temperature (not on its gradient and also not on the mean free path).

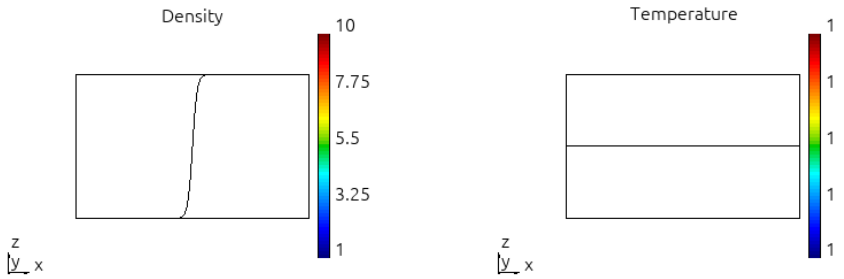

Figure 5: Problem 4 background.

2.8. Implicit fully-discrete scheme

In order to formulate a fully-discrete scheme leaning on an implicit discretization of velocity, the equations (17) and (18) can be expressed with matrices as

$$\begin{aligned}
\mathbf{M}_0 \cdot \frac{\partial \boldsymbol{f}_0}{\partial v} &= \mathbf{D}_0 \cdot \boldsymbol{f}_1 + \mathbf{E}_0^1 \cdot \frac{\partial \boldsymbol{f}_1}{\partial v} + \mathbf{E}_0^2 \cdot \boldsymbol{f}_1 + \mathbf{M}_0 \cdot \frac{\partial \boldsymbol{f}_{\boldsymbol{M}}}{\partial v}, \\
\mathbf{M}_1 \cdot \frac{\partial \boldsymbol{f}_1}{\partial v} &= -\mathbf{D}_1 \cdot \boldsymbol{f}_0 + \mathbf{E}_1^1 \cdot \frac{\partial \boldsymbol{f}_0}{\partial v} + \mathbf{E}_1^2 \cdot \boldsymbol{f}_0 + \mathbf{B} \cdot \boldsymbol{f}_1 + \mathbf{M}_1^t \cdot \boldsymbol{f}_1,
\end{aligned}$$

$$\begin{aligned}
\frac{\mathrm{d}\boldsymbol{f}_0}{\mathrm{d}v} &= \mathbf{M}_0^{-1} \cdot \left(\mathbf{D}_0 + \mathbf{E}_0^2\right) \cdot \left(\boldsymbol{f}_1^n + \Delta v \frac{\mathrm{d}\boldsymbol{f}_1}{\mathrm{d}v}\right) + \mathbf{M}_0^{-1} \cdot \mathbf{E}_0^1 \cdot \frac{\mathrm{d}\boldsymbol{f}_1}{\mathrm{d}v} \\
&\quad + \frac{\partial \boldsymbol{f}_{\boldsymbol{M}}}{\partial v}, \\
\mathbf{M}_1 \cdot \frac{\mathrm{d}\boldsymbol{f}_1}{\mathrm{d}v} &= \left(\mathbf{E}_1^2 - \mathbf{D}_1\right) \cdot \left(\boldsymbol{f}_0^n + \Delta v \frac{\mathrm{d}\boldsymbol{f}_0}{\mathrm{d}v}\right) + \mathbf{E}_1^1 \cdot \frac{\mathrm{d}\boldsymbol{f}_0}{\mathrm{d}v} \\
&\quad + \left(\mathbf{B} + \mathbf{M}_1^t\right) \cdot \left(\boldsymbol{f}_1^n + \Delta v \frac{\mathrm{d}\boldsymbol{f}_1}{\mathrm{d}v}\right),
\end{aligned}$$

$$\frac{\mathrm{d}\boldsymbol{f}_0}{\mathrm{d}v} = \tilde{\mathbf{A}}_0 \cdot \frac{\mathrm{d}\boldsymbol{f}_1}{\mathrm{d}v} + \boldsymbol{b}_0 \left(\boldsymbol{f}_1^n, \frac{\partial \boldsymbol{f}_{\boldsymbol{M}}}{\partial v}\right), \tag{37}$$

$$\left(\mathbf{M}_1 - \Delta v \left(\mathbf{B} + \mathbf{M}_1^t\right)\right) \cdot \frac{\mathrm{d}\boldsymbol{f}_1}{\mathrm{d}v} = \tilde{\mathbf{A}}_1 \cdot \frac{\mathrm{d}\boldsymbol{f}_0}{\mathrm{d}v} + \boldsymbol{b}_1 \left(\boldsymbol{f}_1^n, \boldsymbol{f}_0^n\right), \tag{38}$$

$$\left(\mathbf{M}_1 - \Delta v \left(\mathbf{B} + \mathbf{M}_1^t\right) - \tilde{\mathbf{A}}_1 \cdot \tilde{\mathbf{A}}_0\right) \cdot \frac{\mathrm{d}\boldsymbol{f}_1}{\mathrm{d}v} = \tilde{\mathbf{A}}_1 \cdot \boldsymbol{b}_0 + \boldsymbol{b}_1, \tag{39}$$

[2]

References

[1] J. R. Albritton, E. A. Williams, I. B. Bernstein, Nonlocal electron heat transport by not quite maxwell-boltzmann distributions, Phys. Rev. Lett. 57 (1986) 1887–1890.

[2] V. Dobrev, T. Kolev, R. Rieben, High-order curvilinear finite element methods for Lagrangian hydrodynamics, SIAM J. Sci. Comput. 34 (2012) B606–B641.

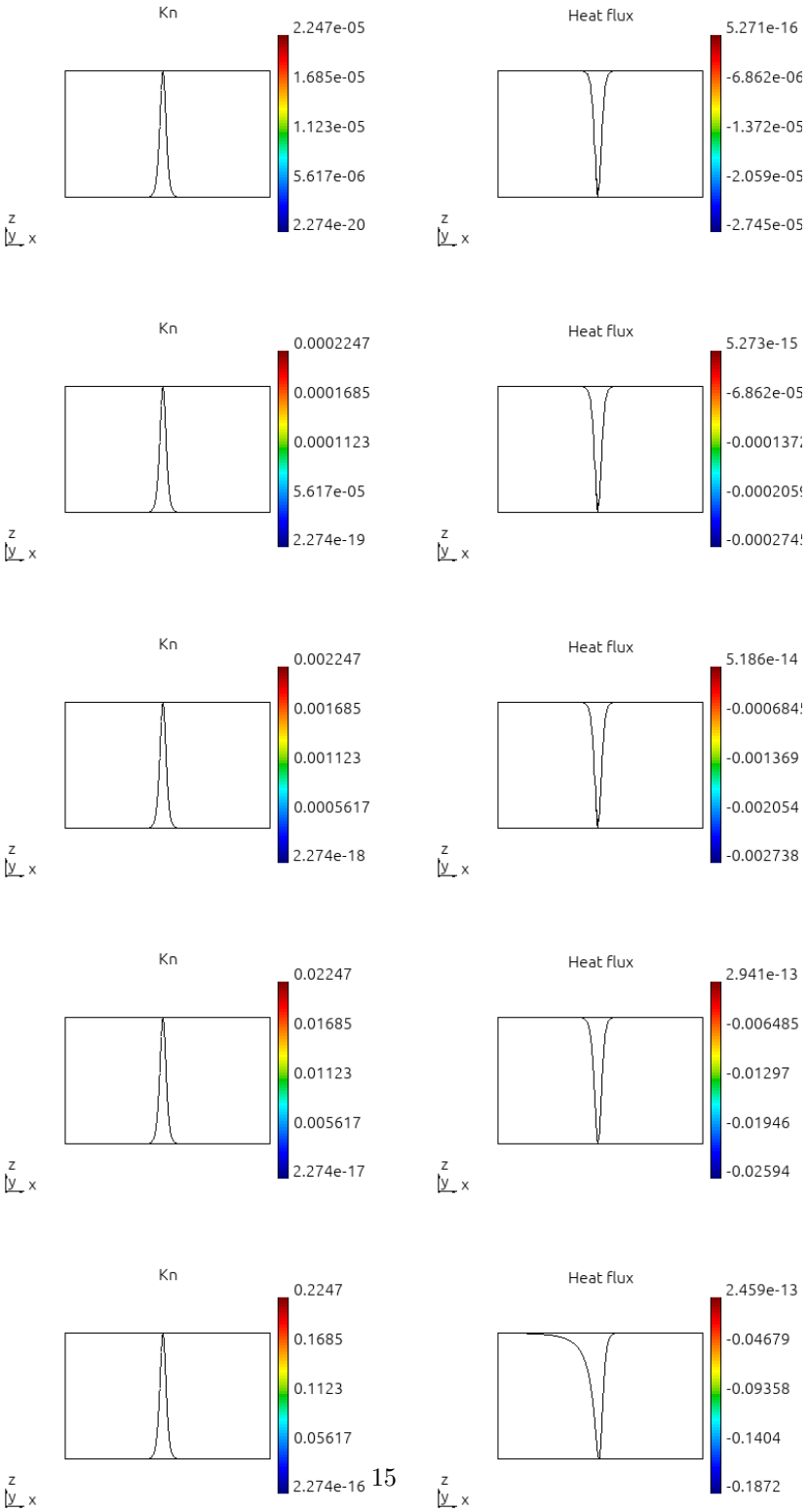

Figure 6: Problem 4 transport.

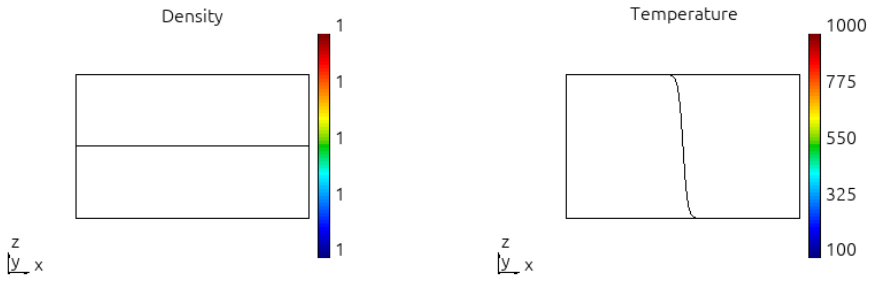

Figure 7: VFP-paper corresponding simulations, ion background density and temperature.

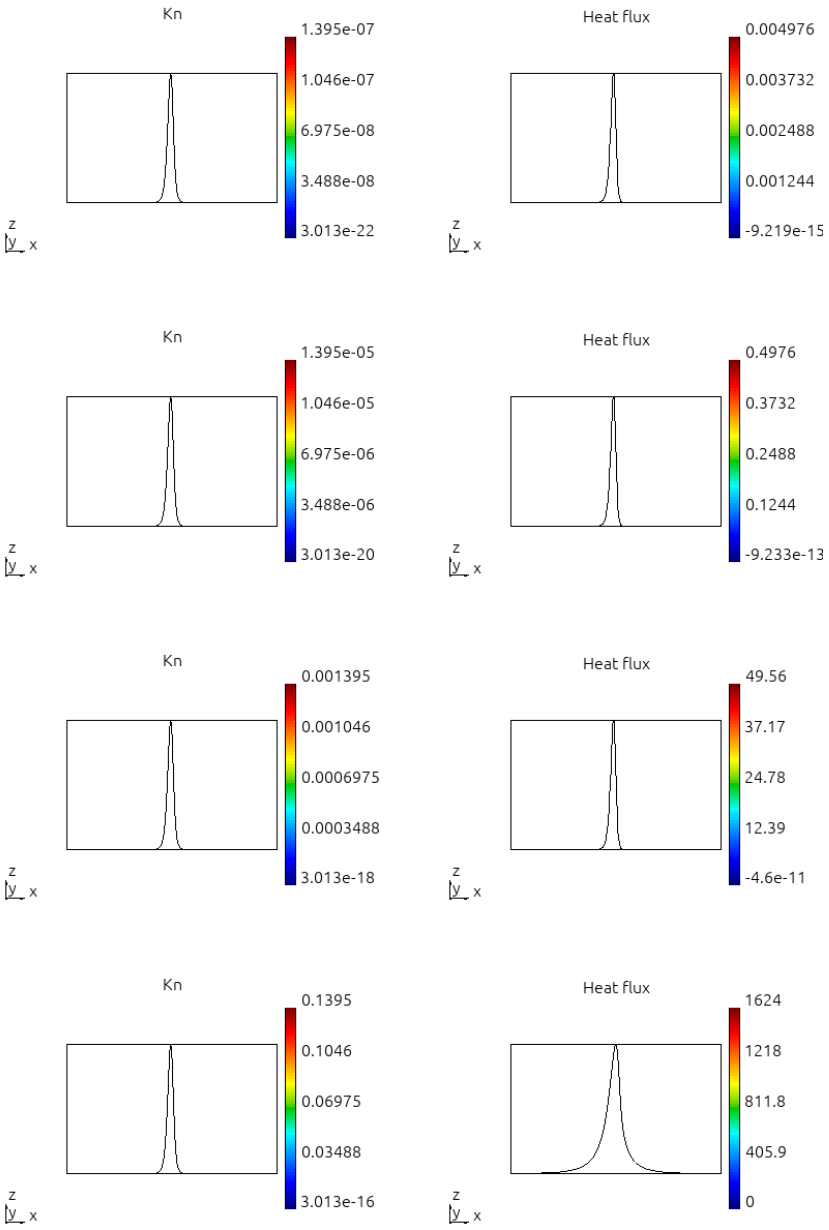

Figure 8: VFP-paper corresponding simulations, Kn spans the interval ($\approx 10^{-7}, \approx 10^{-1}$) where flux goes from diffusive to highly nonlocal.

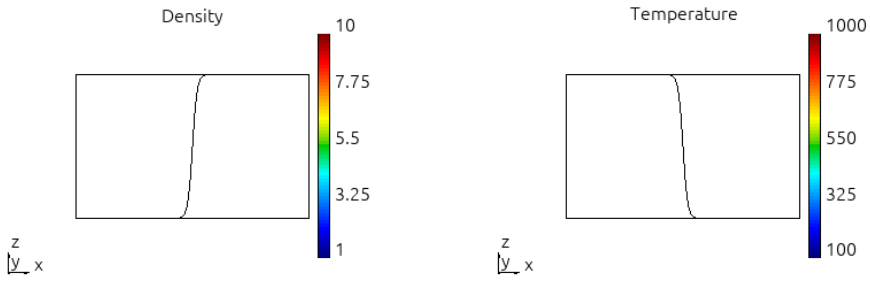

Figure 9: Problem 6 background.

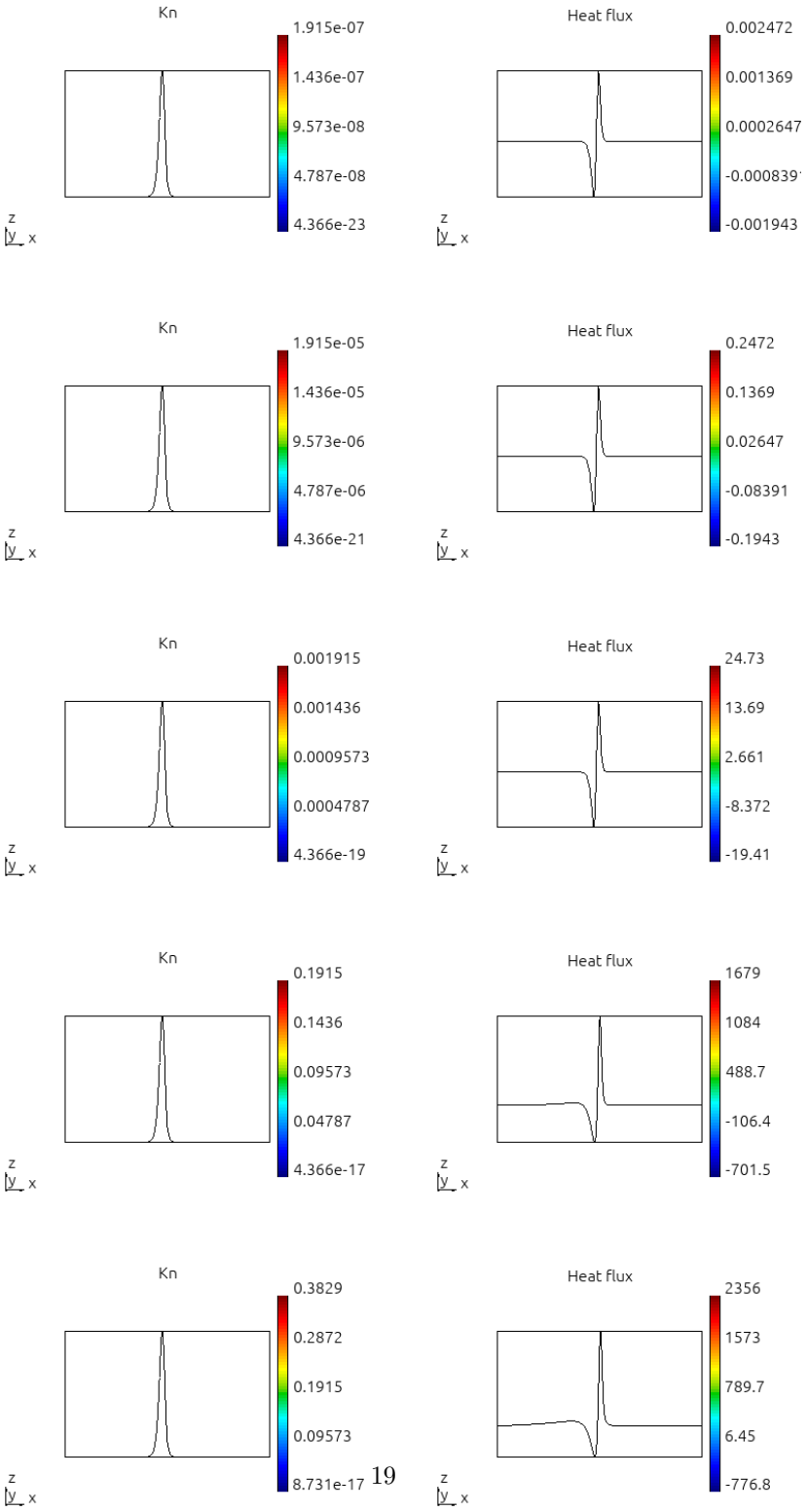

Figure 10: Problem 6 transport.

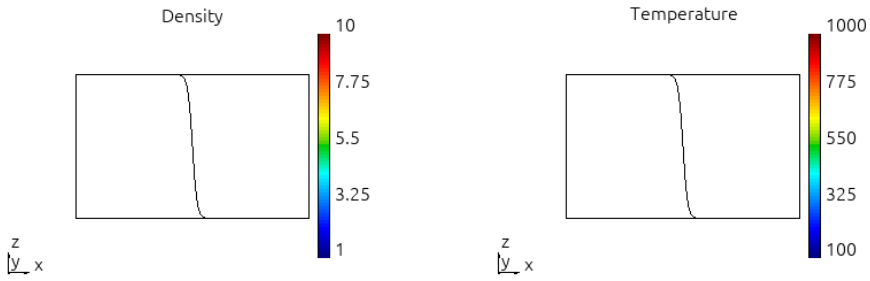

Figure 11: Problem 7 background.

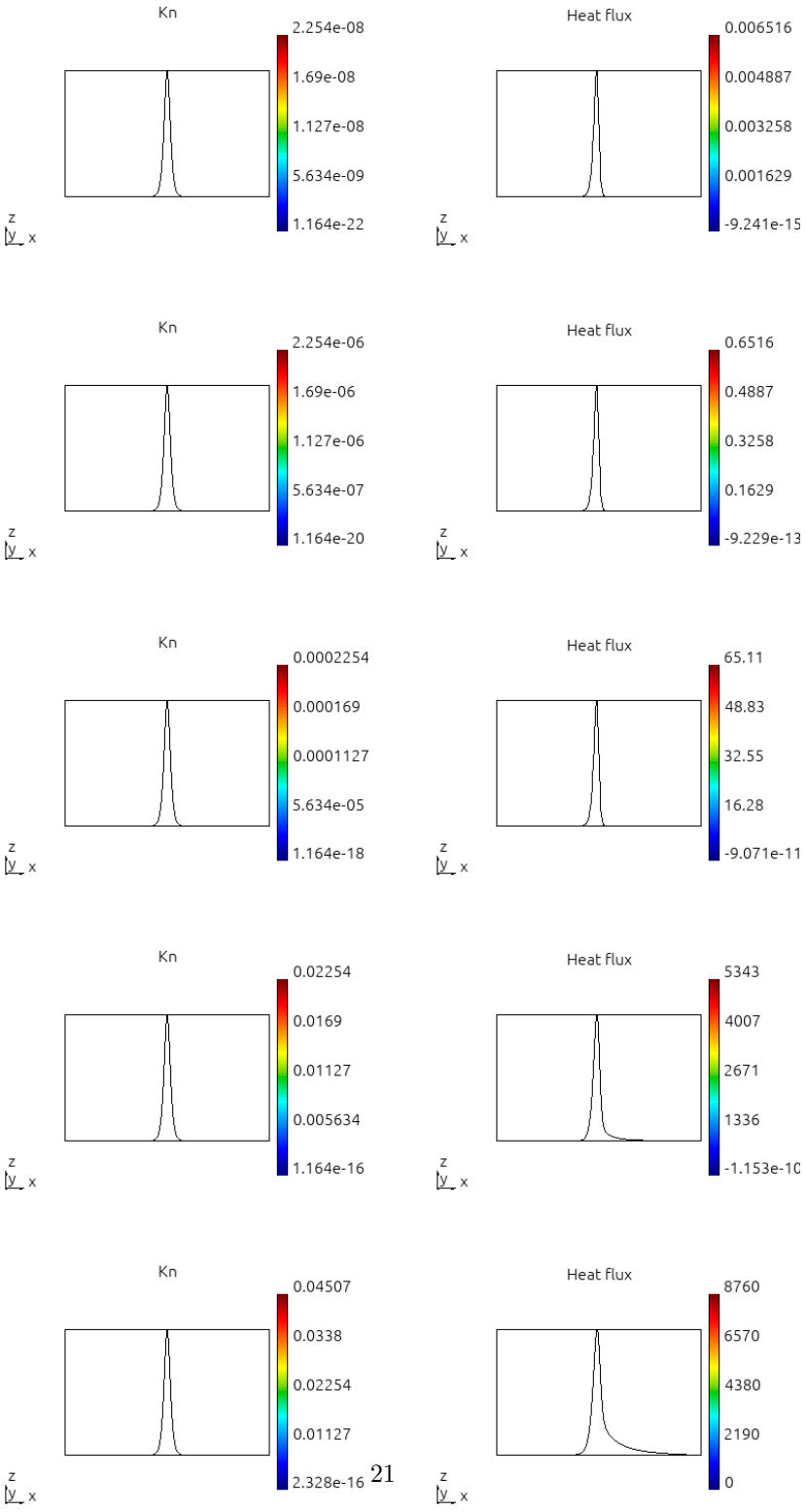

Figure 12: Problem 7 transport.

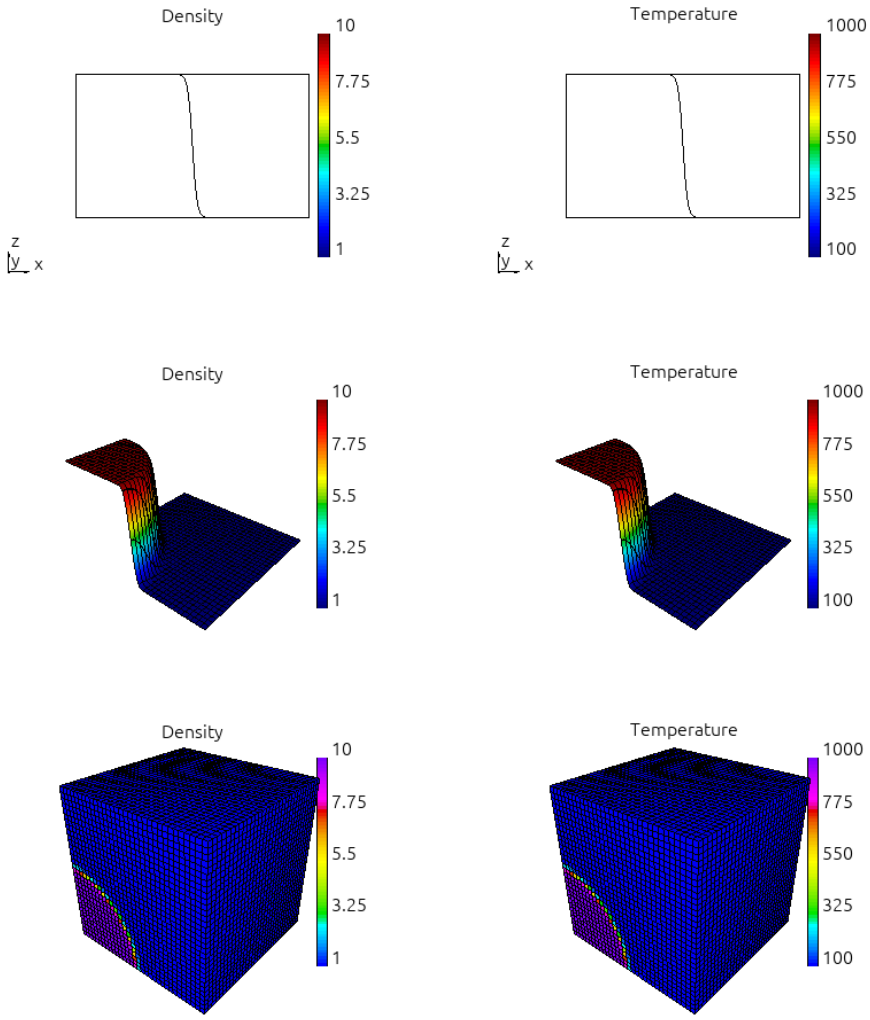

Figure 13: Problem 7 1D/2D/3D background.

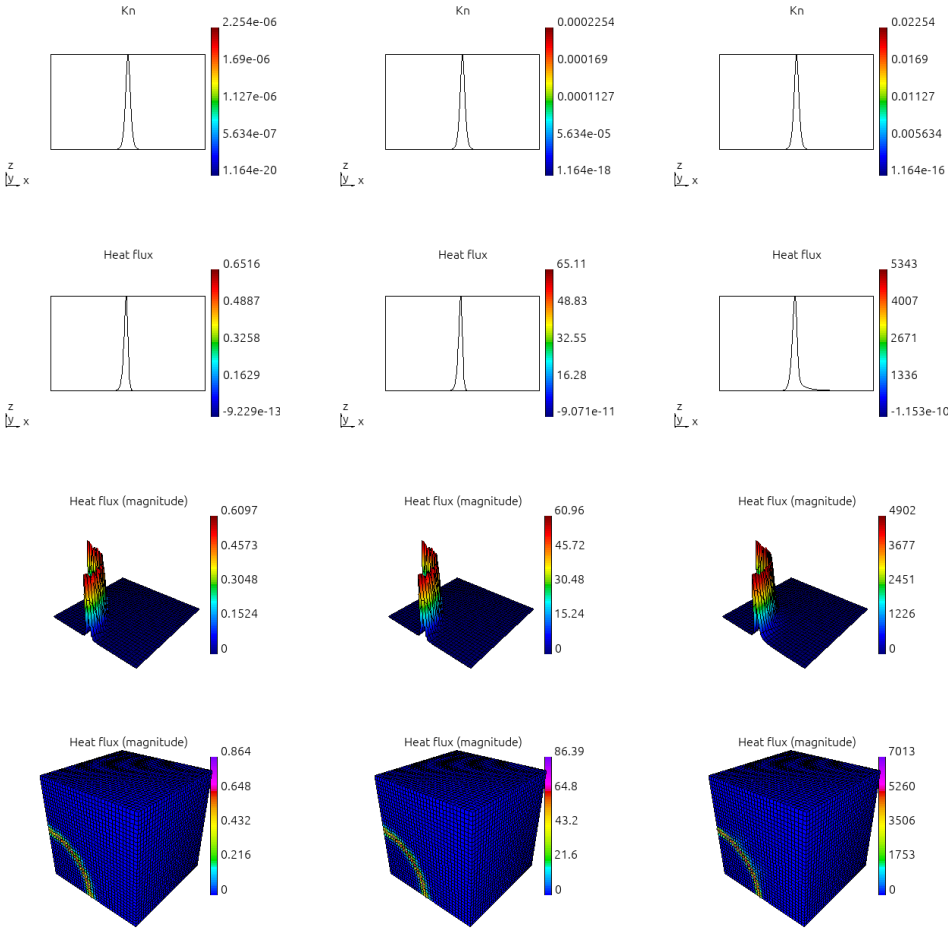

Figure 14: Problem 7 1D/2D/3D transport.

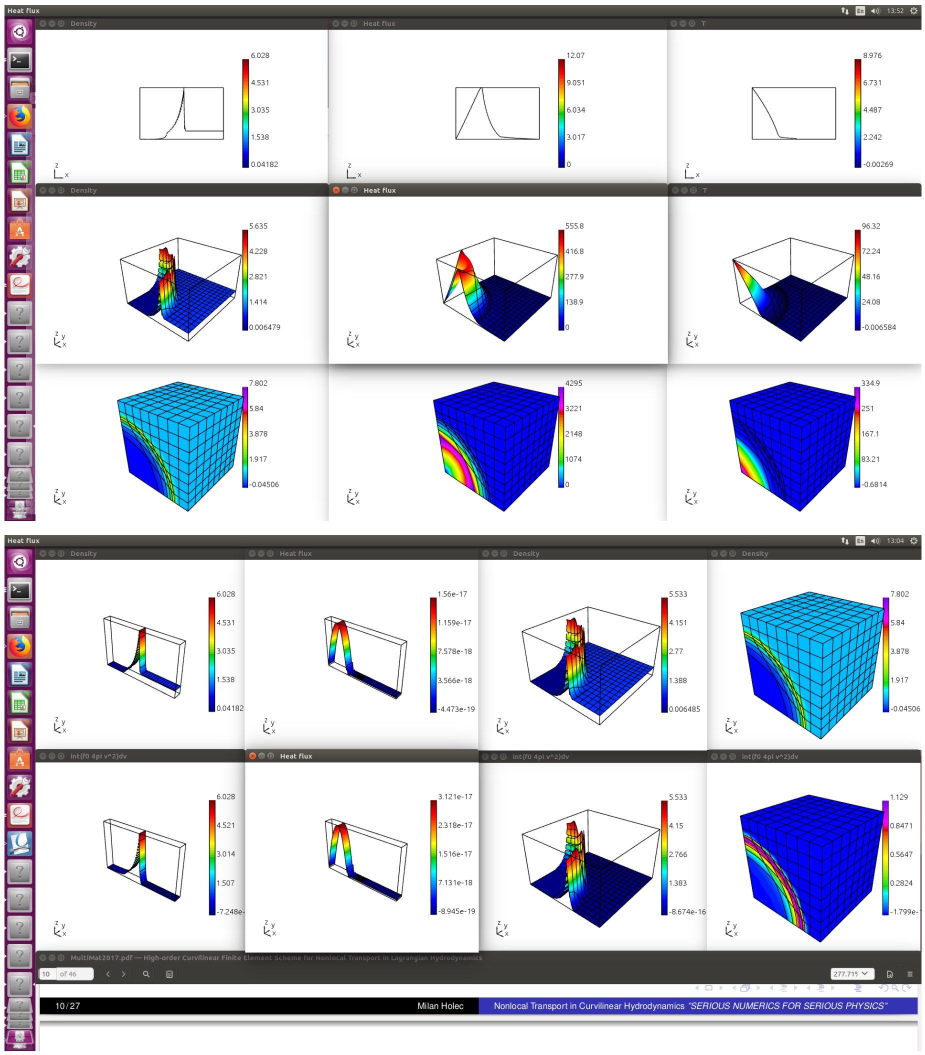

Figure 15: Sedov blast in 1D/2D/3D from δ function hot spot. Shock propagates from left to right. Top raw corresponds to 1D (8858 energy groups) - left: density profile, right: temperature (decreasing from the original hot spot with low temperature in compressed plasma), center: heat flux with its maximum on the start of increase in density decreasing while approaching the shock (NOTICE non-zero flux ahead of the shock). Middle raw corresponds to 2D (4348 energy groups) - left: density, center: heat flux, right: temperature. Bottom raw corresponds to 3D (10030 energy groups) - left: density, center: heat flux, right: temperature.